Free layer versus synthetic ferrimagnet layer auto-oscillations in nanopillars processed from MgO-based magnetic tunnel junctions

S. Cornelissen,[1,2,*] L. Bianchini,[3,4] T. Devolder,[3,4] Joo-Von Kim,[3,4] W. Van Roy,[1] L. Lagae,[1,5] and C. Chappert[3,4]
[1]*IMEC, Kapeldreef 75, B-3001 Leuven, Belgium*
[2]*Department of Electrical Engineering (ESAT), KU Leuven, Leuven, Belgium*
[3]*Institut d'Electronique Fondamentale, CNRS, UMR 8622, 91405 Orsay, France*
[4]*Université Paris-Sud, UMR 8622, 91405 Orsay, France*
[5]*Department of Physics and Astronomy, KU Leuven, Leuven, Belgium*
(Received 13 January 2010; revised manuscript received 16 March 2010; published 7 April 2010)

We study nanopillar spin-torque oscillators processed from low-resistance-area product MgO-based magnetic tunnel junctions. The influence of spin torque can be seen in quasistatic experiments as a strong astroid distortion, consistent with a pure Slonczewski-type spin torque. At microwave frequencies, the spin-torque results in pronounced magnetization auto-oscillations with a clear threshold behavior, though only evidenced in the antiparallel configuration. Two kinds of auto-oscillations are seen depending on the polarity of the voltage applied to the junction. Free layer oscillations require a large easy axis applied field and electrons flowing from the reference layers to the free layer. Acoustic excitation of the reference synthetic ferrimagnet can be seen, provided the electron flow is reversed, indicating a clear similarity with the behavior of conventional all-metallic spin valves. The analysis of the threshold indicates that the amplitude of the spin torque is neither proportional to the current nor to the voltage and it is not accompanied by any significant fieldlike torque.

DOI: 10.1103/PhysRevB.81.144408 PACS number(s): 75.75.−c, 72.25.Pn, 85.75.−d

I. INTRODUCTION

Nanopillars patterned either from all-metallic spin valves or from magnetic tunnel junctions have been thoroughly investigated recently thanks to their potential application in the next generation of magnetic random-access memories[1] or as compact and tunable microwave oscillators.[2] These devices rely on the so-called spin torque,[3,4] i.e., the transfer of spin angular momentum between magnetic layers which results in current-induced torques. For proper applied fields and current densities, the spin torque can manipulate the magnetizations of the layers, inducing hysteretic switching or various kinds of steady-state microwave precession.

Spin-transfer-induced oscillations in spin valves have been extensively reported, both in nanopillar[2] and in point-contact[5] geometries. However, the low magnetoresistance inherent to these all-metallic systems sets a limitation to the microwave power that can be delivered that renders these devices unusable in practical applications. MgO-based tunnel junctions provide larger spin polarization and higher magnetoresistance. Therefore, nanopillars made from MgO-based tunnel junctions are seen as the straightforward solution to meet the demand for higher power. However, auto-oscillations in those systems have been observed only in a few cases,[6,7] and some controversy remains on the required current polarity, the nature of the excited modes,[8,9] the value of the threshold current,[7,10] and the vector nature of the spin torque.[11–13]

In this paper, we study nanopillar spin-torque oscillators processed from low-resistance-area (RA) product MgO-based magnetic tunnel junctions. First, we show that the spin torque acting on the free layer has a pure Slonczewski-type character. We then study in detail the spin-torque-induced microwave auto-oscillations and show a clear similarity with the behavior of conventional all-metallic spin valves. We evidence two kinds of auto-oscillation modes, depending on the polarity of the bias applied to the junction. By the field dependency of their frequencies they can be classified as an oscillation in the free layer and an acoustic oscillation of the synthetic ferrimagnet (SyF) system. Furthermore, our data shows that spin torque in these devices is neither proportional to the current nor to the voltage.

II. EXPERIMENTAL METHODS

Our samples are patterned from low RA product MgO-based magnetic tunnel junctions, deposited in a Singulus Timaris sputtering machine and consisting of Ta 3/CuN 40/Ta 5/PtMn 20/$CoFe_{30}$ 2/Ru 0.8/$CoFe_{20}B_{20}$ 2/MgO 1.3/$CoFe_{20}B_{20}$ 3/Ta 8, where the numbers indicate layer thicknesses in nm. Measurements on micrometer sized tunnel junctions indicate a RA product that varies between 0.9 and 1.4 $\Omega.\mu m^2$. The device to device variations in the RA product are attributed to variations in the thickness of the very thin MgO barrier material as also confirmed by a TEM study, discussed in Sec. IV C. These magnetic junctions are processed into nanopillars with an octagonal 70×130 nm^2 footprint, using methods described in Ref. 14. For the complete set of devices the average parallel and antiparallel resistances are 225 and 270 Ω, respectively, and the average magnetoresistance (MR) ratio is 15%. Assuming the nominal size, this would yield an average $R\times A$ product of 1.8 $\Omega.\mu m^2$, slightly higher than deduced from microscopic junctions. This suggests that the actual dimensions of our devices are smaller by typically 20% than the nominal size. Although we performed our studies on two dozen devices, we shall report in detail only the microwave properties of two specific devices. These two junctions were chosen based on several criteria. These two specific devices show the lowest voltage thresholds, allowing the exploration

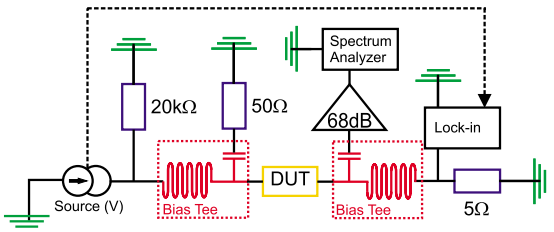

FIG. 1. (Color online) Schematic representation of the experimental setup, the nanopillar under investigation is indicated by device under test (DUT). The DUT is connected to two bias tees. One of the RF sides is amplified and fed to the spectrum analyzer, the other RF signal is terminated in a 50 Ω resistance. Through the dc chain a dc and a small ac bias (333 Hz) are applied by the voltage source, a lock-in amplifier is used to measure the resistance over a 5 Ω shunt resistance.

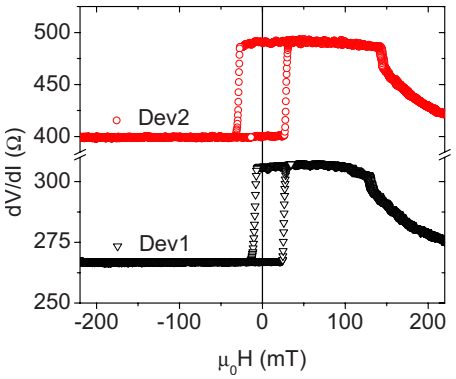

FIG. 2. (Color online) dV/dI loops at zero bias for Dev1 (triangles) and Dev2 (circles), two 70×130 nm^2 octagonal nanopillars.

of a larger parameter space before the occurrence of voltage-induced breakdown of the tunnel junction. Correlated with this, they have higher than average tunnel magnetoresistance (TMR) values (15 and 23%), and also a slightly above average RA product, of respectively 2.1 [device 1(Dev1)] and 3.1 $\Omega.\mu$m^2 [device 2 (Dev2)]. Some results on larger devices, i.e., 100×180 nm^2 will also be reported in Sec. III.

In our measurement setup (Fig. 1) the two electrodes of the nanopillars are connected to coplanar waveguides to allow various electrical measurements. The two waveguides are connected to bias tees allowing dc and rf routing. The dc routes are used for resistance versus field curves up to 250 mT and for differential conductance measurements: an arbitrary waveform generator applies a dc voltage bias with a small superimposed ac modulation at 333 Hz to the device and a shunt resistance (5 Ω) is placed in series in order to measure dI/dV with a lock-in sensitivity. The RF port of the first bias tee is terminated to a perfect (50 Ω) load while the RF port of the other bias tee is sent to a ultrawide band low-noise amplifier feeding a spectrum analyzer with a resolution bandwidth of 5 MHz. The raw-data spectra are translated into power density units taking into account the frequency dependencies of the amplifier gain and of its noise figure. In order to take into account the two impedance mismatches present at the sample plane and at the input stages of the amplifiers, the gain is measured with the device connected but unbiased. Thus, any voltage dependence of the impedance of the tunnel junction is neglected in our data treatment, yielding a possible 20% underestimation of the microwave power at the highest bias voltage investigated here.

Our current convention is that positive voltages correspond to electrons flowing from the SyF to the free layer. Our magnetic field convention is such that positive fields favor antiparallel magnetizations of the free layer and the reference layer of the SyF. Figure 2 shows the hysteresis loops of our two devices. Both loops exhibit clear free layer switching at low fields and a reversible spin-flop transition of the SyF system at large positive field. For Dev1 the free layer coercivities are −9 and +27 mT while for Dev2 they are −28 and +29 mT. The spin-flop fields are, respectively, 130 and 142 mT. Before reporting the details of the experimental results, let us describe some guidelines that can be used for the classification of the spin-torque-induced auto-oscillation modes to be observed. For this purpose, we have calculated in Fig. 3 the eigenfrequencies of a system comprising three macrospins: the free layer and the two SyF layers, the bottom one being exchange biased. The calculation is done following the methods described in Ref. 15 with material parameters determined in a previous study[15,16] and listed in Table I. Three generic types of modes are predicted: the free layer uniform mode (F), the acoustic excitation of the SyF (A) and the optical (O) excitation of the SyF. Free layer excitations have a frequency minimum at the switching field while SyF oscillations (O,A) have extrema at the spin-flop transition. Furthermore, SyF modes can be distinguished by the nature of the extremum, the curvature of the frequency versus field curve and the value of the mode frequency. In addition, the voltage polarity can be used to ascertain the nature of the excitation. Indeed electrons flowing from the SyF to the free layer are expected to destabilize the free layer when in the

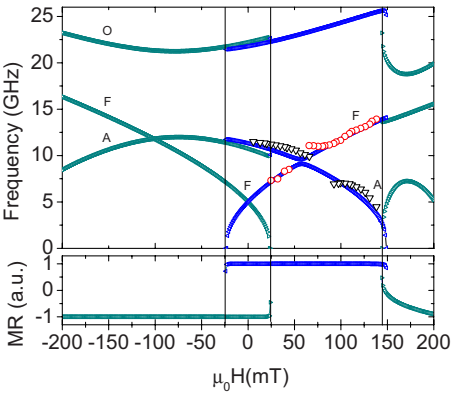

FIG. 3. (Color online) Calculated normalized magnetoresistance loop (bottom) and calculated frequencies of the eigenmodes (top) for a nanopillar in the macrospin approximation. The frequencies are shown for the parallel (triangles pointing right) and antiparallel (triangles pointing left) magnetization states. The labels indicate the free layer (F), acoustic SyF (A) and optical SyF (O) modes. The vertical lines indicate the free layer coercive fields and the spin-flop transition field. For comparison we have superimposed the experimentally found frequencies of Dev1 (downward triangles) and Dev2 (circles).

TABLE I. Magnetic parameters used for modeling the frequencies of the eigenmodes in a three-layer system. M_S indicates saturation magnetization, t the thickness of the layers, and H_k the anisotropy fields for all three layers, the free layer (F), and the two layers of the SyF (SyF1, SyF2). H_{dip} is the F to SyF1 dipolar coupling field, J_{int} the interlayer coupling strength, and H_{eb} the exchange field from the antiferromagnet.

	M_S (T)	t (nm)	$\mu_0 H_k$ (T)
SAF1	1.3	2	0.04
SAF2	1.4	2	0.05
F	1.3	3	0.025
$\mu_0 H_{dip}$ (T)	J_{int} (J/m)	$\mu_0 H_{eb}$ (T)	
0.01	2.9×10^{-4}	−0.12	

AP state. Electrons flowing from free layer to SyF are expected to destabilize the reference layer of the SyF when in the AP configuration.

III. EFFECT OF VOLTAGE ON THE QUASISTATIC PROPERTIES

In order to confirm the expected sign of the spin torque acting on the free layer, we have measured the Stoner asteroids of the free layer under several bias voltages. Because we wanted to explore a large bias interval, resulting in a risk of sample degradation, these measurements were performed on devices of size 100×180 nm^2 instead of on the ones whose auto-oscillation properties have been measured in detail. The asteroids are constructed from resistance versus easy axis field loops measured for several discrete values of applied hard axis fields. In zero bias, the asteroid (Fig. 4) is not centered around zero field but around an easy axis field of 7.5 mT, favoring a P configuration. The zero bias asteroid is not symmetrical, indicating that the AP to P and P to AP reversal paths are significantly different, most probably because of the nonuniform dipolar coupling field with the uncompensated SyF.

Three points are worth noticing in the voltage dependency of the asteroids. First, there is no global displacement of the asteroid as the voltage is increased. Following the analysis method described in Ref. 17, this indicates that there is hardly any current-induced fieldlike torque in our tunnel junctions. We will see hereafter that this statement is further supported by the fact the microwave oscillation frequency is hardly affected by the current flow. Second, the vertical size of the asteroids is not significantly affected by the voltage, which indicates that there is no substantial heating of the junction that would reduce the magnetization or the shape anisotropy field and consequently shrink the asteroid in a rather symmetric manner.[18] Finally, at 200–350 mV of positive voltage bias, a re-entrant zone develops in the left part of the asteroid, indicating a current-induced lowering of the AP to P coercivity. This confirms that a positive voltage bias (electrons flowing from the SyF to the free layer) applies a torque on the free layer that destabilize the AP configuration. The shape of the re-entrant zone is typical[9,17,19] of a spin torque of *pure* Slonczewski vector form, i.e., $m\times(m\times p)$ where m indicates the free layer magnetization direction and p indicates the polarization of the current along the magnetization direction of the top SyF layer. The opposite (negative) voltage impacts the other coercivity (P to AP) but with a much reduced efficiency. We shall see hereafter that this reduced efficiency prevents free layer auto-oscillation in the P configuration. This reduced efficiency at negative voltage also indicates that the spin-torque amplitude is not a linear function of the applied voltage bias but exhibits some curvature in agreement with recent predictions.[20]

IV. MICROWAVE OSCILLATIONS AND THEIR VOLTAGE DEPENDENCE

Microwave oscillations with clear voltage threshold were not obtained when the sample was in the parallel state. Conversely, two very different auto-oscillation behaviors were identified in the AP state, depending on the voltage polarity.

A. Auto-oscillations for negative applied voltages

For negative applied voltages (electrons flowing from free layer to SyF), the majority of the studied devices showed a strong auto-oscillation mode if the system was prepared in the AP configuration. This is for instance the case for Dev1, as shown in Figs. 5(A) and 5(B). The mode exists in a wide

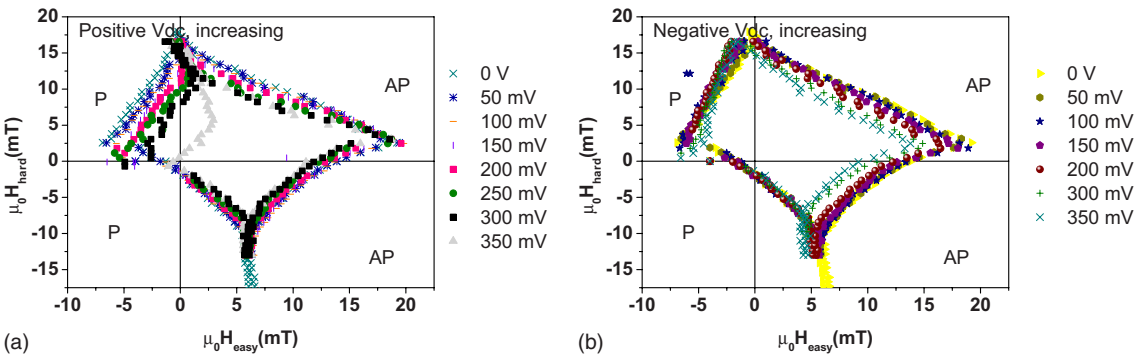

FIG. 4. (Color online) (a) asteroid for positive bias voltages showing the presence of spin torque on the free layer preferring the P state. (b) Asteroid for negative voltages the AP state is slightly preferred due to the opposite sign of the spin torque on the free layer.

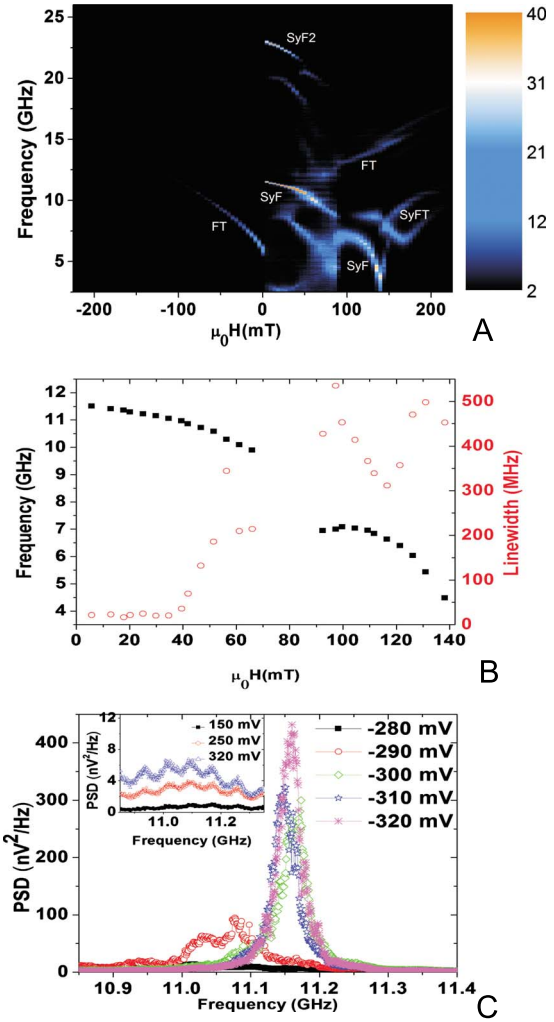

FIG. 5. (Color online) (A) Color plot of the power spectra taken from Dev1 for −340 mV bias as function of the easy-axis-applied field. The different modes are labeled: SyF and SyF2 are the high-power oscillations in the SyF system and its harmonic, FTs are thermal modes in the free layer, SyFT is what we assume to be thermal modes in the SyF system. (B) Center frequency and linewidth as function of the applied field, fitted to A in the region where a high-power oscillation mode is present. (C) Threshold behavior in Dev1 for negative (inset: positive) bias voltage showing a clear threshold accompanied by a nonlinear power increase and linewidth collapse in an externally applied field of 33 mT. Note that the sine-like behavior is an artifact of the measurement system due to imperfect corrections of frequency-dependent impedance mismatches.

range of easy axis fields, typically from just above zero field (5 mT) to the spin-flop field with an interruption between 65 and 90 mT. Close to zero field the mode frequency is typically 11.5 GHz and decreases regularly to some 4.5 GHz at the spin-flop field [Fig. 5(B)]. At the highest investigated voltage (−340 mV), the mode intensity is maximal and the linewidth is minimal near zero field, where the power density exceeds 400 nV^2/Hz and the second harmonic can be detected. The negative voltage mode at 11.15 GHz exhibits a very clear threshold, as illustrated in Fig. 5(C) for an applied field of 33 mT. The mode can hardly be detected for voltages below −280 mV and its amplitude suddenly rises by two orders of magnitude as the voltage is increased from the threshold (−290 mV) up to −320 mV. This power increase is accompanied by a reduction of the linewidth down to 16.5 MHz. Above the threshold this mode shows a tiny blueshift with increasing voltage. This clear threshold behavior is in stark contrast to the positive voltage case [inset of Fig. 5(C)], where no oscillation of interest is present with increasing voltage bias.

Let us now discuss the nature of the excited mode in negative voltage. The value of the experimental frequency, i.e., 11.5 GHz at low field (5 mT) indicates that the observed mode cannot be a free layer mode. Indeed the uniform free layer mode is expected at a much lower frequency (Fig. 3) and the frequency should lower as the applied fields approach the coercivity, which is not observed. Also, the SyF optical mode is expected at significantly higher frequencies. In addition, the curve of the predicted optical-mode frequency versus field has a curvature and a slope that are both opposite to what is observed in the experiments, such that we can exclude an optical SyF mode. In contrast, an acoustic excitation of the SyF can account for our experimental findings and gives reasonable numerical agreement to our measurements (Fig. 3). The easy-axis field dependence of the frequency has the correct slope sign, i.e., it extrapolates toward zero when increasing the field toward the spin-flop field of the SyF. The frequency versus easy axis field has the concave curvature expected for an acoustic excitation (Fig. 3). We conclude that the microwave oscillation seen for negative bias is consistent with an acoustic excitation of the two layers of the synthetic ferrimagnet subsystem. This is consistent with the common belief that, in the AP configuration, spin torque destabilizes the layer toward which the electrons are flowing. However, due to strong interlayer coupling the oscillation induced in the top layer of the SyF persists in both magnetic layers of the SyF.

B. Auto-oscillations for positive applied voltages

We summarize our findings for positive applied voltages here. Compared to the devices showing SyF oscillations, a smaller number of devices showed oscillations with clear threshold behavior and without suffering breakdown. Dev2 is one of them: an oscillation mode for positive applied biases is clearly present for a field direction favoring the AP configuration (Fig. 6). A number of oscillation modes are present in these spectra but only one of them carries a significant power. This main mode is present in a narrow field interval just above the free layer coercivity and also between 65 mT and the spin-flop field [Fig. 6(A)]. The threshold behavior of this mode is illustrated in Fig. 6(C) for an externally applied field of 120 mT, representative of the region where a powerful oscillation is seen. The voltage threshold for this particular oscillation mode lies in between 200 and 250 mV, where a peak suddenly appears at 12.5 GHz with a linewidth of 23 MHz and a clear second harmonic. This peak is very intense compared to our noise floor, in strong contrast to spectra taken with voltages below the threshold.

Let us now discuss the nature of this mode. The experimental frequency resembles that expected for a uniform free

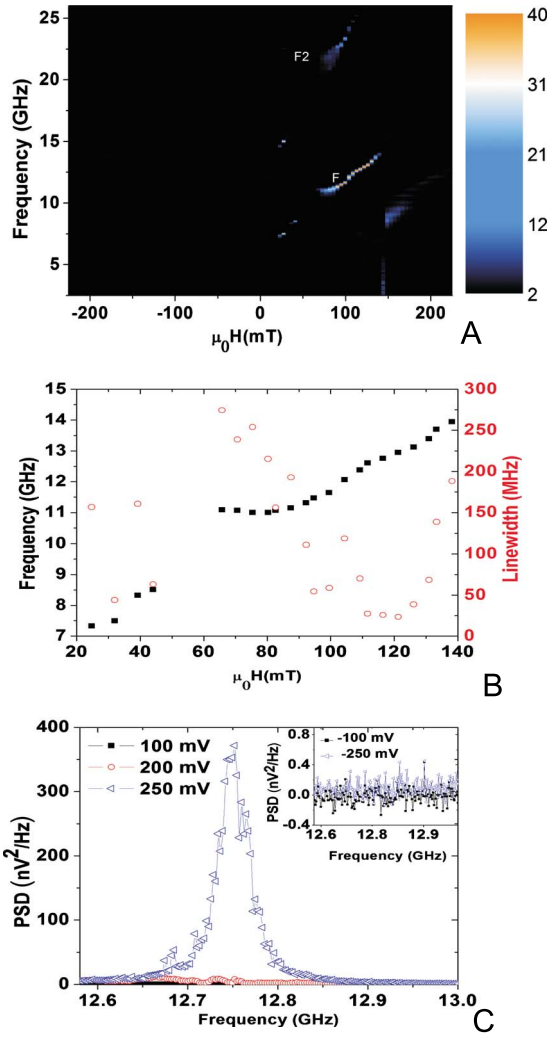

FIG. 6. (Color online) (A) Color plot of the spectra taken from Dev2 for 250 mV bias in function of the applied field along the devices' easy axis. The main free layer mode (F) and its harmonic are labeled (F2) and are the only clearly present modes. (B) Center frequency and linewidth in the field region where the high-power oscillation mode is present. (C) Threshold behavior in Dev2 at 120 mT applied field for positive (inset: negative) bias voltages showing the clear threshold behavior for positive bias.

layer mode (Fig. 3): it increases with the applied field and in addition, it shows a reasonable numerical agreement with the Kittel relation valid for this uniform free layer mode. We conclude that the microwave oscillation seen in positive field is consistent with a quasiuniform free layer excitation, which agrees with the common belief that the positive bias polarity should destabilize the free layer when in the AP configuration.

C. Sample to sample dispersion and significance of the data

From a previous study,[16] performed on stacks with higher and more reproducible RA products due to a longer oxidation time, the variations in size and shape of the nanopillars resulted in resistance variation not bigger than 20% for nanopillars in this size range. Therefore size and shape variations

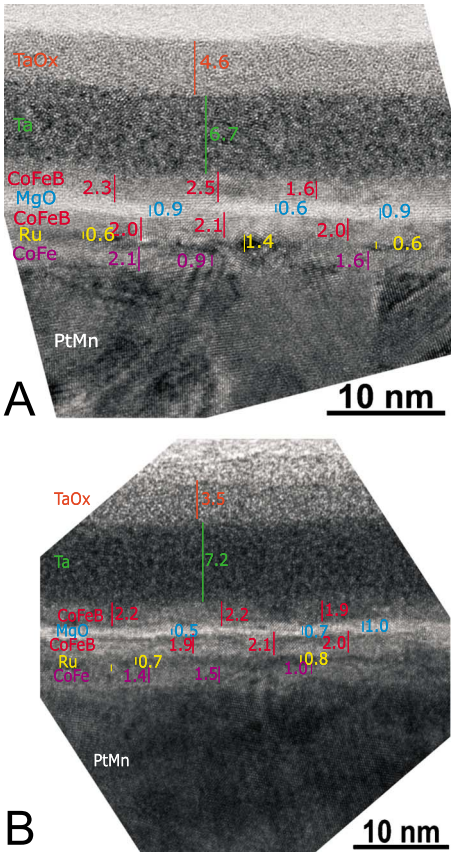

FIG. 7. (Color online) Comparison of barrier thickness uniformity by a transmission-electron microscope study for a standard RA (16 $\Omega.\mu m^2$, panel A) multilayer showing variation in MgO thickness between 0.6 and 0.9 nm and for a low RA (1.4 $\Omega.\mu m^2$, panel B) multilayer showing variation in the MgO thickness between 0.5 and 1.0 nm.

are excluded from being responsible for a preference toward a certain mode. Hence, the resistance and TMR differences in the devices discussed here have to originate elsewhere. When the present low RA multilayers are compared to those with higher RA in a TEM study (Fig. 7), it becomes clear that the difference in oxidation time induces different degrees of roughness and a variation in the MgO thickness across a wafer. From Fig. 2 it is clear that both resistance and TMR in Dev2 are higher than Dev1 so locally the barrier in Dev2 is slightly thicker than in Dev1. A higher TMR implies a better current polarization and consequently more spin-transfer torque for the same current density. However recently it has been stated that thickness variations can change the asymmetry of the spin torque.[20] The induced uncertainty on the reproducibility of the asymmetry of any device can lead to a scattering of the thresholds at different polarities which we believe is the reason for the origin of the different modes in Dev1 and Dev2.

V. DISCUSSION

Several points are worth discussing. Let us first discuss the relation between voltage polarity and the destabilization

of the magnetic layers. We have observed a free layer excitation at positive bias, where electrons flow from the SyF system to the free layer, and a SyF acoustic oscillation at opposite bias, both in the antiparallel configuration. In both cases, the oscillations occur for the voltage polarity expected to yield a spin torque destabilizing the layer system that is effectively oscillating. In that sense, our results indicate that the spin torque in our tunnel junctions is of similar sign as in conventional all-metallic spin valves. Still one point is worth noticing. To get a description of the excitation mode, most studies assume one layer to be static (fixed) when evaluating the effect of spin torque on the dynamics of the other layer. Such reasoning has proven to be insightful but in our case it cannot be applied when the field is near 70 mT. Indeed for that field, there is a crossing of the dispersion relation of the SyF acoustic mode and the free layer mode (Fig. 3). The two modes are hybridized by the interlayer dipolar coupling and neither the free layer nor the SyF could be considered as static if this mode was excited. The destabilizing effect on one layer comes with a stabilizing effect on the other, making the excitation of a hybridized mode difficult. This apparently results in a higher-voltage threshold for microwave excitations: for both positive [Figs. 5(A) and 5(B)] and negative [Figs. 4(A) and 4(B)] applied voltages, the auto-oscillation modes are not present in this field interval up to the breakdown voltage.

Let us now discuss whether the positive and negative thresholds are best defined by currents or by voltage. In most previously reported studies, the measurements were performed in a constant current mode. However since junction breakdown is a voltage mediated mechanism, junctions would always break in the AP state. Like breakdown, spin torque has been stated to be a voltage-mediated phenomena,[20] such that we have chosen to work in constant applied voltage mode. We have never observed microwave oscillations in the P configuration, indicating the voltage thresholds in the P state were systematically higher than the breakdown voltage. Since threshold for free layer oscillation in the P and in the AP configuration are expected to correspond to the same amplitude of spin torque, our results indicate that the spin torque is *not* proportional to the voltage. Nonetheless, spin torque does also not seem to be proportional to the current. Indeed since the resistance of the P state is lower, the same applied voltage yields a larger current, such that if the spin torque was proportional to the current it would be easier to destabilize the layers when in the P configuration, which is opposite to experimental findings. We conclude that the amplitude of the spin torque is neither proportional to the current nor to the voltage in on our tunnel junctions.

As a last comment, we emphasize that our study of the asteroids indicates that spin torque in our devices is not accompanied by a large fieldlike torque. In addition to asteroid measurements, a significant fieldlike torque would shift the mode frequencies with the voltage, which is opposite to experimental findings.

VI. CONCLUSION

In conclusion, our study of nanopillar spin-torque oscillators processed from MgO-based magnetic tunnel junctions clearly showed the presence of Slonczewski-type spin torque acting on the free layer of our system, through strong asteroid distortion for positive voltage biases. In the antiparallel magnetic configuration two excitation modes with clear threshold behaviors and clearly different origins were measured at microwave frequencies. Depending on the polarity of the bias to the junction two kinds of auto-oscillation were witnessed. From the field dependence of the auto-oscillation frequency, we identified free layer oscillations at large easy axis applied field for electrons flowing from the reference layers to the free layer. When reversing the voltage polarity, we saw the acoustical excitation of the synthetic ferrimagnet. The bias polarity that provides selectivity toward a mode recalls a similarity with conventional all-metallic spin valves. Finally, the analysis of the threshold indicated that the amplitude of spin torque in our devices is neither proportional to the current nor to the voltage.

ACKNOWLEDGMENTS

W. Maass (Singulus Technologies AG) is greatly acknowledged for providing low RA MgO-based magnetic tunnel junction stacks. This work has been supported by the European Communities programs IST STREP under Contracts No. IST-016939 TUNAMOS, and "Structuring the ERA" No. MRTN-CT-2006-035327 SPINSWITCH. S. Cornelissen acknowledges IWT flanders for financial support.

*Corresponding author; sven.cornelissen@imec.be

[1] F. J. Albert, J. A. Katine, R. A. Buhrman, and D. C. Ralph, Appl. Phys. Lett. **77**, 3809 (2000).

[2] S. I. Kiselev, J. C. Sankey, I. N. Krivorotov, N. C. Emley, R. J. Schoelkopf, R. A. Buhrman, and D. C. Ralph, Nature (London) **425**, 380 (2003).

[3] J. C. Slonczewski, J. Magn. Magn. Mater. **159**, L1 (1996).

[4] L. Berger, Phys. Rev. B **54**, 9353 (1996).

[5] W. H. Rippard, M. R. Pufall, S. Kaka, S. E. Russek, and T. J. Silva, Phys. Rev. Lett. **92**, 027201 (2004).

[6] A. V. Nazarov, H. S. Cho, J. Nowak, S. Stokes, and N. Tabat, Appl. Phys. Lett. **81**, 4559 (2002).

[7] D. Houssameddine, U. Ebels, B. Dieny, K. Garello, J.-P. Michel, B. Delaet, B. Viala, M.-C. Cyrille, D. Mauri, and J. A. Katine, Phys. Rev. Lett. **102**, 257202 (2009).

[8] D. Houssameddine, S. H. Florez, J. A. Katine, J.-P. Michel, U. Ebels, D. Mauri, O. Ozatay, B. Delaet, B. Viala, L. Folks, B. D. Terris, and M.-C. Cyrille, Appl. Phys. Lett. **93**, 022505 (2008).

[9] Y. Henry, S. Mangin, J. Cucchiara, J. A. Katine, and E. E. Fullerton, Phys. Rev. B **79**, 214422 (2009).

[10] J.-V. Kim, V. Tiberkevich, and A. N. Slavin, Phys. Rev. Lett. **100**, 017207 (2008).

[11] S. Petit, C. Baraduc, C. Thirion, U. Ebels, Y. Liu, M. Li, P. Wang, and B. Dieny, Phys. Rev. Lett. **98**, 077203 (2007).
[12] J. C. Sankey, Y.-T. Cui, J. Z. Sun, J. C. Slonczewski, R. A. Buhrman, and D. C. Ralph, Nat. Phys. **4**, 67 (2008).
[13] H. Kubota, A. Fukushima, K. Yakushiji, T. Nagahama, S. Yuasa, K. Ando, H. Maehara, Y. Nagamine, K. Tsunekawa, D. D. Djayaprawira, N. Watanabe, and Y. Suzuki, Nat. Phys. **4**, 37 (2008).
[14] S. Cornelissen, L. Bianchini, G. Hrkac, M. Op de Beeck, L. Lagae, J.-V. Kim, T. Devolder, P. Crozat, C. Chappert, and T. Schrefl, EPL **87**, 57001 (2009).
[15] A. Helmer, S. Cornelissen, T. Devolder, J.-V. Kim, W. Van Roy, L. Lagae and C. Chappert, Phys. Rev. B **81**, 094416 (2010).
[16] S. Cornelissen, L. Bianchini, A. Helmer, T. Devolder, J.-V. Kim, M. Op de Beeck, W. Van Roy, L. Lagae and C. Chappert, J. Appl. Phys. **105**, 07B903 (2009).
[17] T. Devolder, J.-V. Kim, C. Chappert, J. Hayakawa, K. Ito, H. Takahashi, S. Ikeda, and H. Ohno, J. Appl. Phys. **105**, 113924 (2009).
[18] M. Jamet, W. Wernsdorfer, C. Thirion, D. Mailly, V. Dupuis, P. Mélinon, and A. Pérez, Phys. Rev. Lett. **86**, 4676 (2001).
[19] J. Z. Sun, Phys. Rev. B **62**, 570 (2000).
[20] I. Theodonis, N. Kioussis, A. Kalitsov, M. Chshiev, and W. H. Butler, Phys. Rev. Lett. **97**, 237205 (2006).